Cureus Journal of Engineering

Open Access Original Article

A Comparative Study on Structural, Crystallographic and Microstructural Properties of Nano-TiO2 Intermixed and Surface-Coated Portland Cement Mortars

Received 08/06/2024
Review began 08/09/2024
Review ended 08/24/2024
Published 09/09/2024

DOI:
https://doi.org/10.7759/s44388-024-00403-y

Avinash Reddy [1] , Sri Chandana Panchangam Prof. [2]

1. Civil, JNTUA, Ananthapur, IND 2. Civil Engineering, Annamacharya Institute of Technology and Sciences, Kadapa, IND

Corresponding author: Sri Chandana Panchangam Prof., srichandanaloka@gmail.com

Abstract

The present study aimed to investigate the influence of minimal nano TiO_2 (NT) on the microstructural and crystallographic analysis of various application methods, such as intermixing, fresh cast coating, and hardened coating, for ordinary Portland cement (OPC 53 grade) mortar. X-ray diffraction coupled with Rietveld refinement was employed to quantify the crystal phases. The structural parameters, such as unit cell dimensions, lattice parameters, volumes, and crystallographic integrity of the OPC mortar discs with and without NT were examined. Additionally, scanning electron microscopy was employed to analyze the microstructural morphology and hydration products with NT integration. The results showed that the hardened NT coating led to the most refined structural model with the shortest bond distances and smallest polyhedral volumes in the crystal structure. This suggests that the denser packing of atoms with stronger atomic interactions between the smaller NT particles within the cement matrix created a more compact and uniform microstructure. This microstructure improvement, which is evident by less calcium hydroxide formation and denser calcium-silicate hydrate formation, improved the overall performance of the OPC cement mortar with minimal NT dosages.

Categories: Sustainable Technologies, Nano Materials, Nanotechnology
Keywords: self-cleaning, nano tio2 (nt), crystallography, microstructure, csh

Introduction

Nano TiO_2 (NT) as a photocatalyst has gained significant attention in recent years as an additive/supplement for developing self-cleaning cementitious materials due to its unique properties, such as a high refractive index, stability, nontoxicity, cost-effectiveness, and its self-cleaning, antimicrobial, and depolluting properties [1-6]. Titanium dioxide is primarily composed of three crystal structures: brookite, anatase, and rutile [4,7,8]. NT, as a photocatalyst in cement, improved the depollution characteristics and aesthetic durability, reduced atmospheric pollutants, and enhanced the self-cleaning photocatalytic performance. Rhodamine B (RhB) dye was used to assess the self-cleaning performance [9]. In a study in warm subhumid climates, coating mortars with 3% synthesized NT demonstrated superior degradation efficiency under visible light and an improved self-cleaning effect under weather exposure, and it significantly enhanced the compressive strength of the mortars [10]. Moreover, the photocatalytic performance of mesoporous TiO_2 films enables the efficient oxidation of nitrogen oxide, leading to efficient air purification through the adsorption of intermediate products and nitric acid [11]. The photocatalytic performance of self-cleaning cement is also improved by incorporating 10% calcined dolomite into a mixture of 87% clinker and 3% microsized TiO_2, which also reduces costs and nanotoxicity [12]. Interestingly, on cement substrates, TiO_2 composite films doped with P25 via a sol-gel method showed excellent photocatalytic performance for removing organic pollutants, such as RhB, from surface water [13].

In one study, NT- and NT-SiO_2-coated Portland cement concrete blocks effectively degraded organic dyes and enhanced photocatalytic performance [14], while in another study, nano-SiO_2-NT (NST) reduced the concentrations of NO and SO_2 in roadside environments [15]. Graphene/TiO_2-coated cement mortars also demonstrated strong photocatalytic efficiency for air purification and self-cleaning [16]. Furthermore, the photocatalytic activity of cement mortar containing 2% Ag-TiO_2 under UV light is the highest, while cement mortar containing 5% Ag-TiO_2 exhibits the highest activity when exposed to solar light [17]. Additionally, modified TiO_2 photocatalysts (TiO_2-N, C) with commercial gypsum also showed improved photocatalytic performance and enhanced compressive strength, indicating that these materials have great potential as self-cleaning building/construction materials [18]. NT and low-calcium fly ash in cementitious composites improved their ability to remove NOx pollutants through photocatalytic processes and enhanced their self-cleaning and air-purifying capabilities [19].

The integration of nanotitanium particles in cement-based materials significantly enhanced the mechanical properties of the materials. The toughness, durability, and tensile and flexural strengths of the cement-based material were significantly enhanced by the incorporation of 3% NT, which also decreased the permeability and water absorption. This could be attributed to the nucleation effect, enhanced calcium-silicate hydrate (CSH), and filling and interlocking effect of the NT [20]. The mechanical characteristics of self-compacting concrete specimens (SCCs) increased with the integration of NT up to 4 wt% [21]. In another study, reinforced nano-SiO_2-coated TiO_2 (NSCT) with reactive powder concrete enhanced the flexural and compressive strengths, acted as a nanofiller in the cement matrix, demonstrated a pozzolanic effect, and contributed to the compact cement matrix [22].

In another study, the addition of 3% NT to 20% fly ash improved the compressive strength more effectively than the addition of 10% or 30% fly ash and increased the exothermic hydration rate, which may promote early hydration and expedite the formation and precipitation of hydration products [23]. Furthermore, incorporating NT into fly ash (30%) blended cement mortars at a 3% dosage by weight of cement resulted in increased compressive and flexural strengths compared to those of the reference specimen. This enhancement accelerated the rate of hydration of both the cement and the fly ash and promoted additional nucleation sites for the precipitation and formation of C-S-H gel [24]. In another investigation, cement paste modified by NT agglomerates (60-75 nm) with a small quantity of NT (0.9 wt%) increased the compressive strength and flexural strength after 28 days by 14.15% and 16.12%, respectively. This could be attributed to the small amount of NT particles and great dispersion, which act as nuclei for cement hydration and increase the degree of hydration. Moreover, internal microcracks and microporosity reduced and significantly enhanced the content of cement hydration products (C-S-H) [25]. The optimal dosage of NT depends on factors such as the agglomeration degree, size, and water/cement ratio, and excessive NT can restrict cement hydration and reduce strength [26].

X-ray diffraction (XRD) combined with Rietveld refinement analysis is a powerful technique that enables a detailed analysis of the crystal structure of material by minimizing the disparity between the observed and calculated diffraction patterns using a least squares fitting approach [4,27,28], and the same approach was applied in the quantitative analysis of cement-based materials and their hydration characteristics [4,29-31]. VESTA is a powerful tool used for 3D visualization and analysis of crystal structures and various other structural properties of materials and their crystallography, enabling the Rietveld refinement process using XRD [4].

To comprehend the effect of NT particles on interactions with OPC 53-grade,a combination of Rietveld refinement and XRD was used to analyze the crystal structure of material at the atomic and nanoscale levels. This study provides insights into the interaction between NT and cement particles, certain modifications in the crystal lattice and the orientation of the NT particles within the cement matrix. The primary objective of this research is to (i) assess the effect of minimal NT on various application methods, such as intermixing, fresh coating, and hardened coating, of OPC mortar utilizing Rietveld refinement in conjunction with XRD; (ii) examine the structural parameters, such as the lattice parameters, volumes, and crystallographic integrity, of the prepared NT-modified ordinary Portland cement mortar discs through intermixed and surface-coated methods; (iii) investigate the effect of NT on the microstructural characteristics of OPC cement mortar on intermixed and surface-coated samples; (iv) investigate the influence of NT on the bond distances between cations (Ca, Si) and anions (O) as well as the average bond distances and polyhedral volumes of calcium ions (Ca1, Ca2) and silicon ions (Si1) surrounding oxygen (O) atoms in OPC mortar discs.

Materials And Methods

Materials

Nano TiO_2: NT particles in the anatase form, with a size ≤ 25 nm, a specific surface area of 50 m^2/g, and a purity of 99.5%, were obtained from Sigma Aldrich (Degussa P25) for the present study.

Cement: OPC 53 grade conforming to IS 269:2015 [32] from the Zuari Cement brand was used.

Fine aggregates: The fine aggregates used in this study were obtained from local river sand, confirming zone II of IS:383-2016 [33]. The specific gravity and fineness modulus of the fine aggregates were determined to be 2.60 and 3.11, respectively. In addition, the river sand had loose and bulk densities of 1550 kg/m^3 and 1735 kg/m^3, respectively.

Water: Potable water meeting the standards of IS:456-2000 [34] was used for the present investigation.

Experimental Procedure

To examine the structural, microstructural, and crystallographic changes in the cement matrix modified with NT, the parameter TSA (the amount of NT applied to the disc surface area in cm^2) [4] was applied (shown in equation 1). Table *1* shows the detailed proportions of the mix. The detailed experimental flow chart is shown in Figure *1*.

TSA (mg/cm^2) = Amount of TiO_2 / Surface area of the square disc ....(1)

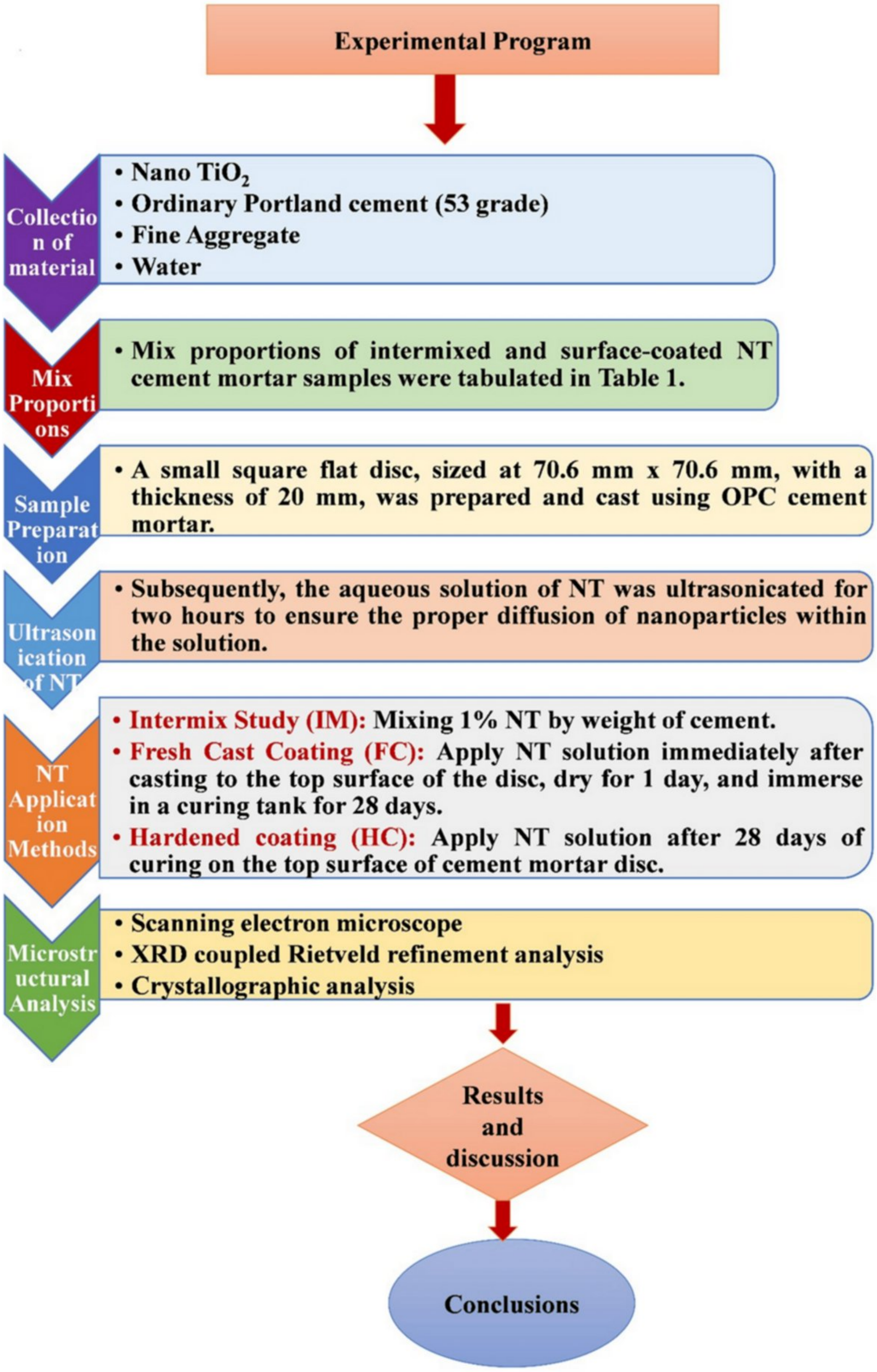

FIGURE 1: Experimental flow chart of the impact of NT on intermixed and surface-coated OPC cement mortar samples

Microstructural analysis

SEM

A JEOL IT500 scanning electron microscope equipped with an Ametek EDAX (Energy Dispersive X-Ray Analysis) detector was used to examine the morphology and hydration products of NT-doped ordinary Portland cement (53 grade) mortar discs for the intermixed and surface-coated specimens.

XRD Coupled with Rietveld Analysis

Rietveld refinement was applied to the OPC specimens modified with NT using Pan Analytical Xpert High Score Plus and EXPO-2014 software.

Crystallographic Analysis

Crystallographic analysis was performed using VESTA software to confirm specific atoms and bonds within the crystal structure.

Intermix (IM) Proportions							
Cement (g)	FA (g)	w/c ratio	NT Addition (% wt)	NT (mg)	Size of Disc (mm)	Surface Area of Specimen (cm^2)	TSA (mg/cm^2)
55	165	0.45	1	55	70.06 × 70.06 × 20	50	1.1
NT coating on FC (Fresh cast coat) cement mortars							
55	165	0.45	-	50	70.06 × 70.06 × 20	50	1
NT coating on HC (Hardened coat) cement mortars							
55	165	0.45	-	50	70.06 × 70.06 × 20	50	1

TABLE 1: Mix proportions of intermixed and surface-coated NTs (ordinary Portland cement-53 grade)

Results

Rietveld and Crystallographic Analysis of NT-modified Cement Mortar

The Rietveld refinement process is a powerful technique conducted with the help of EXPO-2014 [4,35] software and is used to analyze powder diffraction data to determine the crystal structure of materials. The Rietveld parameter Rexpected (Rexp), a theoretical value used to assess the agreement between the observed diffraction pattern (blue color) and a calculated pattern (red color) based on a proposed crystal structure model, is shown in Figure *2*, and lower Rexp values indicate better agreement [4,27,28]. The Rexp values were 5.37, 5.33, 5.16, and 4.91 for TSA 0, TSA IM, TSA FC, and TSA HC, respectively. D-statistics represent the error indices and quantify the overall deviation between the observed and calculated diffraction patterns. Lower D-statistics values indicate a smaller error, which indicates a better fit. On the other hand, weighted D-statistics take into account the intensity of each data point when calculating the error. Table *2* shows a decrease in Rexpected, D-statistics, and weighted D-statistics for intermixed and surface-coated samples compared to the control mortar specimen, and moreover, the surface treatments enhanced the fit between the calculated and observed diffraction patterns. Consequently, this implies that these treatments result in structural improvements at the molecular level, which are able to enhance the overall accuracy of the Rietveld refinement model. As compared to the other samples, TSA HC1 mg/cm^2 indicates the lowest values in Rexp, D-statistics, and weighted D-statistics, which would suggest that this particular treatment is very effective in improving the overall quality of the fit as well as material properties and induces considerable structural improvements that contribute to enhancing the structural integrity of the OPC matrix. Overall, these hypotheses support these surface modifications' positive impact on the material's properties, including the fit of the diffraction data. Therefore, these structural improvements are crucial for understanding the impact of NT on the crystallographic and microstructure properties of OPC, aiding in the optimization of cementitious materials for various applications.

Sample (mg/cm^2)	Rexpected (Rexp)	D-Statistics	Weighted D-Statistics
TSA 0	5.37	0.05659	0.06106
TSA 1.1 IM	5.33	0.05545	0.05272
TSA 1 FC	5.16	0.04787	0.03761
TSA 1 HC	4.91	0.03608	0.03437

TABLE 2: Rietveld refinement parameters cement mortar specimens with varying surface treatment methods

Table *3* shows the different samples of OPC mortar discs doped with minimal NT for intermixing, fresh coating, and hardened coating, with the number of atoms, bonds, and polyhedra determined using VESTA [4]. Polyhedra demonstrate the geometric shapes formed by connecting atoms in the crystal structure. The crystallographic information file (Ca_2O_4 Si) from the crystallographic database serves as a baseline for atomic structure observation. TSA 0 refers to the control sample without the addition of NT to the cement mortar disc and comprises 60 atoms, 72 bonds, and 12 polyhedra units. Similarly, the TSA IM, TSA FC, and TSA HC samples also showed the same number of atoms, bonds and polyhedra, indicating that the addition of NT did not alter the fundamental composition of OPC at the atomic or molecular level. This finding implies that the structural integrity and the crystalline nature of the material remain consistent in all NT application methods and are unaffected by the influence of NT in the cement matrix. This likely enhances the material characteristics of the cementitious material without compromising its essential crystallographic integrity.

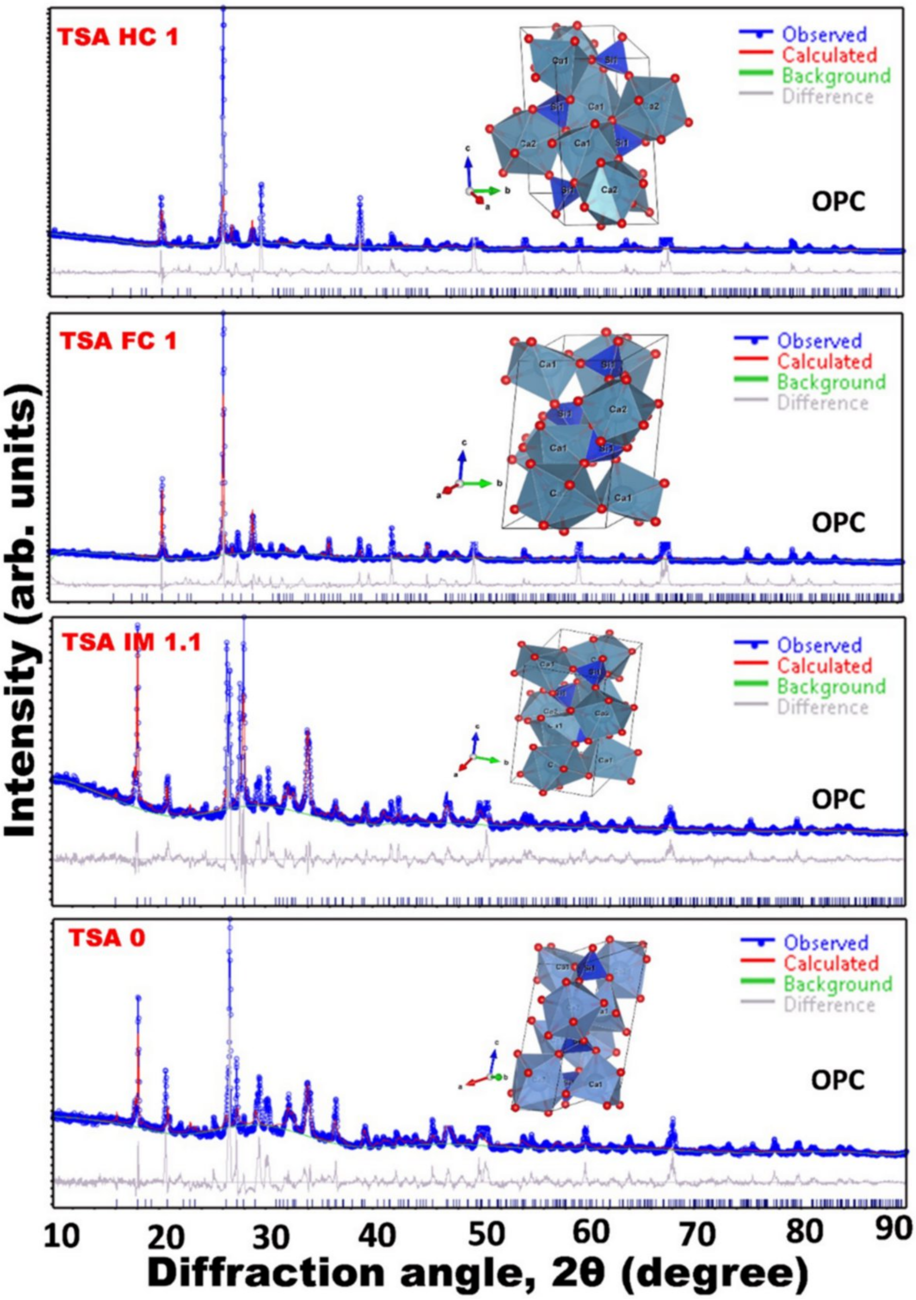

FIGURE 2: Rietveld analysis of OPC (a) TSA 0 (without NT), (b) TSA IM 1.1, (c) TSA FC 1, and (d) TSA HC 1

OPC				
Sample (mg/cm^2)	Atoms	Bonds	Polyhedral	CIF
TSA 0	60	72	12	Ca_2 O_4 Si
TSA 1.1 IM	60	72	12	
TSA 1 FC	60	72	12	
TSA 1 HC	60	72	12	

TABLE 3: Crystal structure parameters determined by VESTA software

Discussion

Impact of NT on the Crystal Structure Parameters of OPC Mortar

Table 4 shows the lattice parameters of the OPC mortar with and without NT. Reference sample TSA 0 without any NT addition had a volume of 350.498 Å³, indicating a monoclinic crystal system with space group P 21/c. The samples with intermixed NT, fresh coats, and hardened coats of NT had reduced volumes of 346.914 Å³, 349.685 Å³, and 343.904 Å³, respectively, compared to those of TSA 0 with the same crystal system and space group. Compared with those of the reference sample, the hardened coating of minimal NT resulted in a decrease in volume of 1.88%, suggesting a denser packing of atoms, possibly due to stronger interactions between the smaller NT particles and the cement matrix and significant structural rearrangement within the crystal structure. Similarly, for the intermixed sample, slight compaction or denser packing and rearrangement of the crystal structure with a reduction in volume of 1.02% were observed, while the freshly coated sample showed minimal structural changes with a 0.23% reduction in volume and did not significantly alter the unit cell structure. The β angle slightly decreased from 117.65° to 117.30°, which is consistent with the observed changes in the unit cell dimensions and volumes.

Lattice Parameters (OPC)										
Sample (mg/cm^2)	a(Å)	b(Å)	c(Å)	V(Å)^3	α(⁰)	β(⁰)	γ(⁰)	Crystal system	Space group	CIF
TSA 0	5.540	6.770	10.550	350.498	90.00	117.65	90.00	Monoclinic	P 21/c	Ca_2 O_4 Si
TSA IM	5.515	6.750	10.510	346.914	90.00	117.54	90.00	Monoclinic	P 21/c	
TSA FC	5.530	6.760	10.540	349.685	90.00	117.44	90.00	Monoclinic	P 21/c	
TSA HC	5.500	6.740	10.440	343.904	90.00	117.30	90.00	Monoclinic	P 21/c	

TABLE 4: Lattice parameters of the intermixed and surface-coated OPC samples with and without NT

Comparison and Crystal Structure Analysis of Ca1, Ca2, and Si1

Table 5 shows the variation in the interatomic bond distances between the cations (Ca, Si) and anions (O) of the NT-modified OPC mortar of the intermixed and surface-coated OPC materials. The crystal structure coordination (Ca1, Ca2, Si1, and O) of the NT-modified OPC mortar is shown in Figure 3. A crystal structure with two different coordination environments for calcium ions, Ca1 and Ca2, is shown in Figure 4 for the hardened coating surface (TSA HC), along with the average bond lengths, polyhedral volumes, and coordinates (*x*, *y*, *z*) for the oxygen atoms surrounding the calcium ions. The average shorter bond length (2.4443 Å) and smaller polyhedral volume (15.3972 Å3) for Ca1 suggest stronger interactions and a more compact arrangement of atoms compared to Ca2 ions in the TSA HC. The greater increase in the polyhedral volume (26.9214 Å3) of Ca2 is assumed to be due to a more expansive coordination environment or greater spatial freedom. The oxygen coordinates (*x*, *y*, *z*) for Ca1 also suggest that the oxygen atoms are relatively close to the Ca1 ion, indicating a more compact polyhedral volume than that of Ca2. In the case of Si1-O, as shown in Figure 5, the shorter average bond length (1.6316 Å) and the polyhedral volume (2.2201 Å³) in the TSA HC suggest highly compact and stable tetrahedral units around the silicon atoms, enhancing the crystal structure stability and rigidity of the material. Similarly, Table 6 describes the average bond lengths and polyhedral volumes of the Ca1-O, Ca2-O, and Si1-O bonds of TSA

0, TSA IM, and TSA FC, respectively. Overall, the minimal intermixing (TSA IM) sample showed a slight compaction of the structure, while the minimal fresh coating (TSA FC), similar to the reference sample (TSA 0) with minimal structural changes and minimal hardened coating (TSA HC), exhibited the most compact dense structure with the shortest bond lengths and smallest polyhedral volumes in the crystal structure.

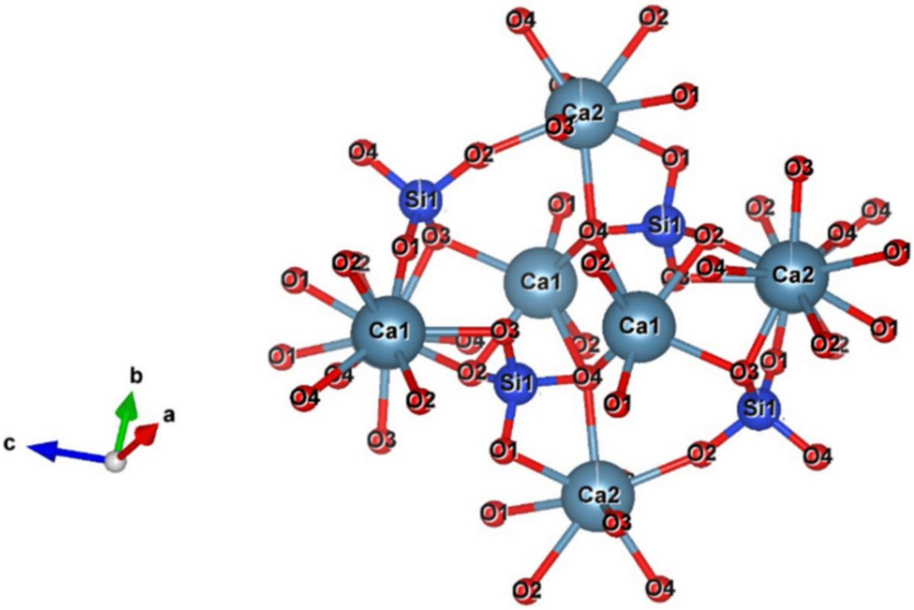

FIGURE 3: Crystal structure coordination (Ca1, Ca2, Si1, and O) of the NT-modified OPC mortar

Type	Cation	Anion	Distance (TSA 0) (Å)	Distance (TSA IM) (Å)	Distance (TSA FC) (Å)	Distance (TSA HC) (Å)	Observations
Ca-O	Ca1	O1	2.228	2.221	2.224	2.218	Slight decrease in bond length after NT intermixing and coating, suggests minor structural changes
Ca-O	Ca1	O3	2.522	2.513	2.520	2.497	Noticeable decrease in hardened layer coat, indicates significant impact on bond
Ca-O	Ca1	O2	2.424	2.417	2.427	2.415	Minimal variations with stable bond length
Ca-O	Ca1	O4	2.657	2.649	2.654	2.641	Consistent small decrease in bond length and significant reduction in TSA HC followed by IM
Ca-O	Ca1	O2	2.557	2.548	2.552	2.541	Small decrease in bond length
Ca-O	Ca1	O4	2.370	2.359	2.366	2.353	Slight consistent reduction in TSA HC followed by IM and FC
Ca-O	Ca2	O3	2.397	2.388	2.393	2.382	Minor decreases in bond length, suggests small change in bond orientations
Ca-O	Ca2	O3	2.391	2.384	2.390	2.384	Stable bond lengths
Ca-O	Ca2	O1	2.680	2.668	2.674	2.652	Significant reduction in HC sample
Ca-O	Ca2	O4	2.463	2.457	2.465	2.450	Small reductions
Ca-O	Ca2	O2	2.659	2.650	2.654	2.643	Consistent reduction
Ca-O	Ca2	O2	2.419	2.409	2.414	2.395	Slight decrease with the significant reduction in HC.
Ca-O	Ca2	O4	2.631	2.623	2.629	2.619	Consistent decrease
Ca-O	Ca2	O1	2.447	2.440	2.450	2.431	Slight decrease
Si-O	Si1	O1	1.619	1.614	1.616	1.611	Slight decrease
Si-O	Si1	O3	1.632	1.627	1.634	1.627	Minor variations
Si-O	Si1	O4	1.659	1.654	1.659	1.646	Slight decrease with most in HC
Si-O	Si1	O2	1.657	1.6492	1.6527	1.642	Slight decrease with most in HC

TABLE 5: Variation in the interatomic bond distances between cations (Ca, Si) and anions (O) in the NT-modified OPC mortar for various application methods

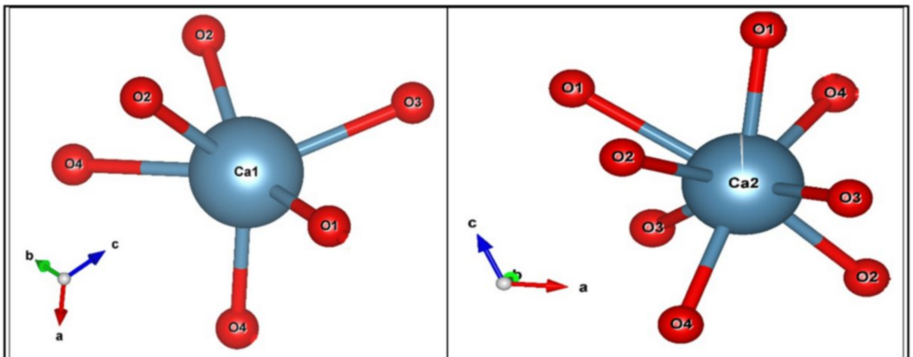

(a) For TSA HC Sample Average Bond Length: 2.4443 Å Polyhedral Volume: 15.3972 Å³				(b) For TSA HC Sample Average Bond Length: 2.4944 Å Polyhedral Volume: 26.9214 Å³			
	x	y	Z		X	y	Z
O1	0.72450	0.48580	0.94070	O4	-0.27270	-0.17150	0.07330
O3	0.67190	0.25130	0.69180	O2	-0.15030	-0.33200	0.36330
O4	0.27270	0.17150	0.92670	O3	-0.32810	0.24870	0.19180
O2	0.84970	-0.16800	0.86330	O1	-0.27550	0.01420	0.44070
O4	0.72730	-0.17150	1.07330	O3	0.32810	-0.25130	0.30820
O2	1.15030	0.16800	1.13670	O1	0.27550	-0.01420	0.55930
-	-	-	-	O2	0.15030	0.16800	0.13670
-	-	-	-	O4	0.27270	0.32850	0.42670

FIGURE 4: Structural parameters of octahedral (a) Ca1 and its distance (Å) to O1, O2, O3, and O4; (b) Cubic Ca2-O1, O2, O3, and O4 in the TSA HC

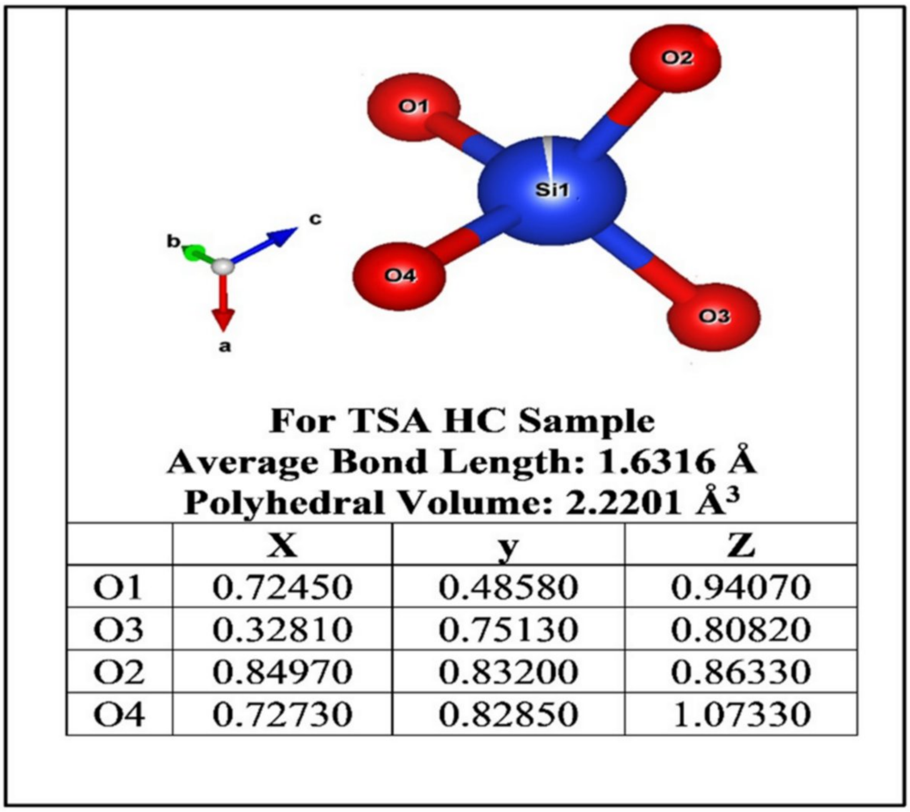

FIGURE 5: Structural parameters of tetrahedral (a) Si1 and its distance (Å) to O1 and O2 in TSA HC

Type	TSA0 (Ca1-O)	TSA 0 (Ca2-O)	TSA0 (Si1-O)	TSA IM (Ca1-O)	TSA IM (Ca2-O)	TSA IM (Si1-O)	TSA FC (Ca1-O)	TSA FC (Ca2-O)	TSA FC (Si1-O)
Average Bond Length (Å)	2.4596	2.5108	1.6417	2.4512	2.5023	1.6361	2.4573	2.5087	1.6404
Polyhedral Volume ($Å^3$)	15.6924	27.4376	2.2627	15.5319	27.1571	2.2395	15.6560	27.3740	2.2574

TABLE 6: Comparison of average bond lengths and polyhedral volumes with and without NT in OPC mortar

Microstructural analysis

SEM

The SEM micrographs illustrate the microstructural differences in the cement mortar samples with and without NT, as shown in Figure 6. Figure 6(a) (TSA 0) shows that calcium hydroxide (CH) has a large, crystalline structure, while CSH is fibrous. In the intermixed sample (TSA IM) shown in Figure 6(b), a slight reduction in CH and a denser, more uniform presence of CSH were observed. Figure 6(c) shows that the application of a fresh coat of NT (TSA FC) on the cement mortar surface enhanced CSH formation, with dense packing and the presence of CH. The hardened coating of NT (TSA HC) in Figure 6(d) resulted in the densest and most uniformly distributed CSH, with less CH. These observations suggest that NT integration, whether it is intermixed, freshly coated, or hardened, refines the microstructure by promoting denser CSH gel formation and reducing CH crystals [4,36-40]. Overall, incorporating minimal NT into various application methods in cement mortar in the present study positively impacts the microstructural characteristics of cement mortar, contributing to its overall performance enhancement.

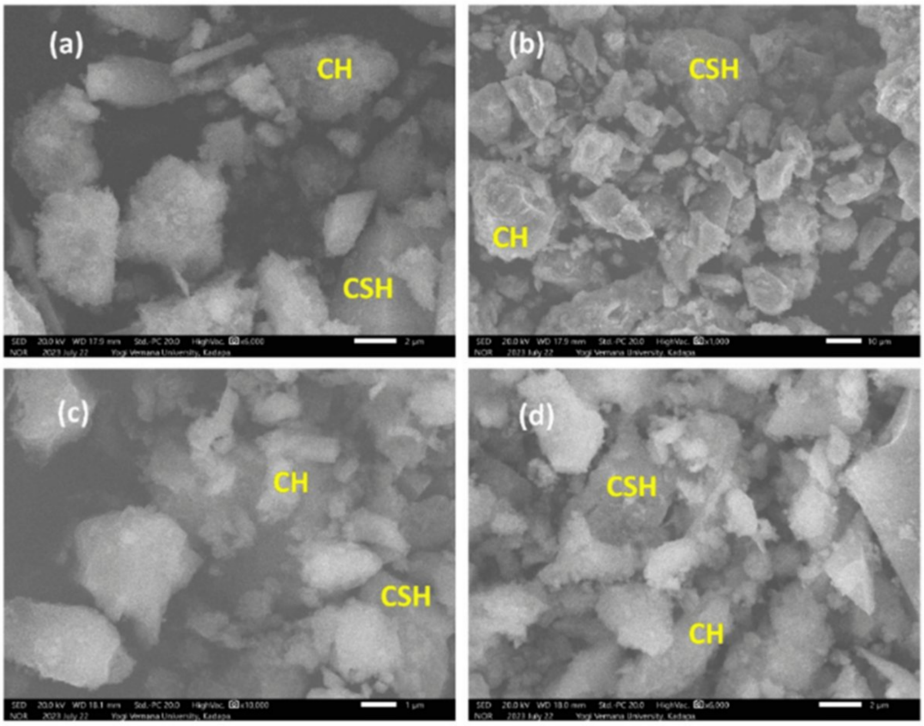

FIGURE 6: SEM micrographs of OPC (a) TSA 0, (b) TSA IM, (c) TSA FC, and (d) TSA HC

Conclusions

The key conclusions of the XRD-coupled Rietveld refinement and crystallographic analysis of the NT-modified cement mortar were as follows:

The reduction in Rexp values for both the fresh surface coat (TSA FC) and hardened coat (TSA HC) samples demonstrated a more substantial agreement between the observed and computed diffraction patterns compared to the reference (TSA 0) and intermixed (TSA IM) specimens. The TSA HC sample exhibited the lowest Rexp value, which can be attributed to the improvement in the structural integrity of the OPC matrix.

The incorporation of NT and their crystallographic consistency, such as the number of atoms, bonds, and polyhedral units, suggest that the fundamental composition of OPC at the atomic and molecular levels remained unchanged.

All NT-modified samples experienced a decrease in unit cell volume, with a significant reduction in volume of 1.88% in the NT-modified hardened coating (TSA HC). This suggests a denser packing of atoms, which is attributed to the stronger interaction between the smaller NT particles within the cement matrix.

In the TSA HC sample, the average shorter bond length and lower polyhedral volume for Ca1 indicate a more compact arrangement of atoms and stronger interactions than for Ca2 ions.

The addition of NT, particularly in hard coat applications, results in a more homogeneous and dense packing of CSH and a decrease in CH. This microstructure improvement, which is evident by less CH formation and denser CSH production, improves the overall performance of the cement mortar.

Additional Information

Author Contributions

All authors have reviewed the final version to be published and agreed to be accountable for all aspects of the work.

Concept and design: Sri Chandana Panchangam Prof., Avinash Reddy

Acquisition, analysis, or interpretation of data: Sri Chandana Panchangam Prof., Avinash Reddy

Drafting of the manuscript: Sri Chandana Panchangam Prof., Avinash Reddy

Critical review of the manuscript for important intellectual content: Sri Chandana Panchangam Prof., Avinash Reddy

Supervision: Sri Chandana Panchangam Prof.

Disclosures

Human subjects: All authors have confirmed that this study did not involve human participants or tissue. **Animal subjects:** All authors have confirmed that this study did not involve animal subjects or tissue. **Conflicts of interest:** In compliance with the ICMJE uniform disclosure form, all authors declare the following: **Payment/services info:** All authors have declared that no financial support was received from any organization for the submitted work. **Financial relationships:** All authors have declared that they have no financial relationships at present or within the previous three years with any organizations that might have an interest in the submitted work. **Other relationships:** All authors have declared that there are no other relationships or activities that could appear to have influenced the submitted work.

Acknowledgements

This article being submitted is an invitation received from the organizers of the conference “Emerging Multifunctional Materials and Devices for Sustainable Technologies (IEMDST-2024)” organized by the Department of Physics NIT Warangal in association with the National Institute of Technology, Goa

References

1. Janczarek M, Klapiszewski Ł, Jędrzejczak P, et al.: Progress of functionalized TiO2-based nanomaterials in the construction industry: a comprehensive review. Chem Eng J. 2022, 430:132062 . 10.1016/j.cej.2021.132062.
2. Jin Q, Ma H: Nano TiO2-engineered cementitious materials with self-cleaning properties. Nanotechnol Civil Infrastruct. 2023, 1:191-209. 10.1016/B978-0-12-817832-4.00006-7
3. Wei Y, Wu Q, Meng H, et al.: Recent advances in photocatalytic self-cleaning performances of TiO2-based building materials. RSC Adv. 2023, 13:20584-97. 10.1039/D2RA07839B.
4. Reddy NA, Panchangam SC: Evaluation of self-cleaning performance of TiO 2 -intermixed and TiO 2 -coated cement mortars under natural sunlight. J Sustain Cem-Based Mater. 2024, 13:1032-49. 10.1080/21650373.2024.2346890
5. Rosa RH, Silva RS, Nascimento LL, et al.: Photocatalytic and antimicrobial activity of TiO2 films deposited on fiber-cement surfaces. Catalysts. 2023, 13:861. 10.3390/catal13050861
6. Bersch JD, Flores-Colen I, Masuero AB, et al.: Photocatalytic TiO2-based coatings for mortars on facades: a review of efficiency, durability, and sustainability. Buildings. 2023, 13:186. 10.3390/buildings13010186
7. Li JG, Ishigaki T, Sun X: Anatase, brookite, and rutile nanocrystals via redox reactions under mild hydrothermal conditions: phase-selective synthesis and physicochemical properties. J Physical Chem. 2007, 111:4969-76. 10.1021/jp0673258
8. Borisov SV, Magarill SA, Pervukhina NV : Crystallographic analysis of TiO2 polymorphism (Brookite, Anatase, Rutile. J Struct Chem. 2019, 60:1783-1789. 10.1134/S0022476619110118
9. Folli A, Pade C, Hansen TB, et al.: TiO2 photocatalysis in cementitious systems: insights into self-cleaning and depollution chemistry. Cem Concr Res. 2012, 42:539-48. 10.1016/j.cemconres.2011.12.001
10. Kuk-Dzul L, Jiménez LF, Vega-Azamar RE, et al.: Photocatalytic activity and self-cleaning effect of coating mortars with TiO2 added: practical cases in warm sub-humid climates. Materials. 2023, 17:190. 10.3390/ma17010190
11. Kalousek V, Tschirch J, Bahnemann D, et al.: Mesoporous layers of TiO2 as highly efficient photocatalysts for the purification of air. Superlattices Microstruct. 2008, 44:506-13. 10.1016/j.spmi.2007.12.004
12. Ratan JK, Saini A, Verma P: Microsized-titanium dioxide based self-cleaning cement: incorporation of calcined dolomite for enhancement of photocatalytic activity. Materials Research Express. 2018, 5:115509. 10.1088/2053-1591/aadd87
13. Guo X, Rao L, Wang P, et al.: Photocatalytic properties of P25-doped TiO 2 composite film synthesized via sol-gel method on cement substrate. J Environ Sci. 2018, 66:71-80. 10.1016/j.jes.2017.05.029
14. Jafari H, Afshar S: Improved photodegradation of organic contaminants using nano-TiO2 and TiO2-SiO2 deposited on Portland Cement Concrete Blocks. Photochem Photobiol. 2016, 92:87-101. 10.1111/php.12554
15. Lee JW, Lee SH, Jang YI, et al.: Evaluation of reducing NO and SO2 concentration in nano SiO2-TiO2 photocatalytic concrete blocks. Materials. 2021, 14:7182. 10.3390/ma14237182
16. Pei C, Zhu JH, Xing F: Photocatalytic property of cement mortars coated with graphene/TiO2 nanocomposites synthesized via sol-gel assisted electrospray method. J Cleaner Product. 2021, 279:123590. 10.1016/j.jclepro.2020.123590
17. Wu L, Pei X, Mei M, et al.: Study on photocatalytic performance of Ag/TiO2 modified cement mortar. Materials. 2022, 15:4031. 10.3390/ma15114031
18. Janus M, Zatorska J, Zając K, et al.: The mechanical and photocatalytic properties of modified gypsum materials. Mater Sci Eng B . 2018, 236:1-9. 10.1016/j.mseb.2018.11.015
19. Xu M, Clack H, Xia T, et al.: Effect of TiO2 and fly ash on photocatalytic NOx abatement of engineered cementitious composites. Constr Build Mater. 2020, 236:117559. 10.1016/j.conbuildmat.2019.117559
20. Ma B, Li H, Mei J, et al.: Effects of nano-TiO2 on the toughness and durability of cement-based material. Adv Mater Sci Eng. 2015, 2015:1-10. 10.1155/2015/583106

21. Nazari A, Riahi S: The effect of TiO2 nanoparticles on water permeability and thermal and mechanical properties of high strength self-compacting concrete. Mater Sci Eng A. 2010, 528:756-63. 10.1016/j.msea.2010.09.074
22. Han B, Li Z, Zhang L, et al.: Reactive powder concrete reinforced with nano SiO2-coated TiO2. Constr Build Mater. 2017, 148:104-12. 10.1016/j.conbuildmat.2017.05.065
23. Ma B, Li H, Li X, et al.: Influence of nano-TiO2 on physical and hydration characteristics of fly ash-cement systems. Constr Build Mater. 2016, 122:242-53. 10.1016/j.conbuildmat.2016.02.087
24. Ng DS, Paul SC, Anggraini V, et al.: Influence of SiO2, TiO2 and Fe2O3 nanoparticles on the properties of fly ash blended cement mortars. Constr Build Mater. 2020, 258:119627. 10.1016/j.conbuildmat.2020.119627
25. Feng LC, Gong CW, Wu YP, et al.: The study on mechanical properties and microstructure of cement paste with nano-TiO2. Adv Mater Res. 2012, 629:477-81. 10.4028/www.scientific.net/amr.629.477
26. Meng T, Yu Y, Qian X, et al.: Effect of nano-TiO2 on the mechanical properties of cement mortar. Constr Build Mater. 2012, 29:241-45. 10.1016/j.conbuildmat.2011.10.047
27. Rietveld HM: A profile refinement method for nuclear and magnetic structures. J Appl Cryst. 1969, 2:65-71. 10.1107/S0021889869006558
28. Ankoji P, Rudramadevi BH: Structural and luminescence properties of Eu3+ doped LaAlO3 nanophosphors by hydrothermal method. J Mater Sci Mater Electronics. 2018, 30:2750-62. 10.1007/s10854-018-0551-6
29. Grazziotin-Soares R, Nekoofar MH, Davies T, et al.: Crystalline phases involved in the hydration of calcium silicate-based cements: semi-quantitative Rietveld X-ray diffraction analysis. Australian Endodontic J. 2019, 45:26-32. 10.1111/aej.12226
30. Aranda MAG, De la Torre AG, León-Reina L: Rietveld quantitative phase analysis of OPC clinkers, cements and hydration products. Rev Mineral Geochem. 2012, 74:169-209. 10.2138/rmg.2012.74.5
31. Tlamsamania D, Ait-Mouha M, Slassi S, et al.: Quantitative phase analysis of anhydrous clinker Portland using Rietveld method. Rev Inorganic Chem. 2022, 43:189-99. 10.1515/revic-2022-0005
32. Indian Standards: IS 269:2015 ‘ordinary Portland cement-specification’ (sixth revision). Bureau of Indian Standards, New Delhi; 2015.
33. Indian Standards: Indian Standards. IS:383-2016 ‘coarse and fine aggregate for concrete-specification’ (third revision). Bureau of Indian Standards, New Delhi; 2016.
34. Indian Standards: IS 456:2000, Plain and reinforced concrete-Code of Practice. Fourth revision. Bureau of Indian Standards, New Delhi; 2000. 1:
35. Altomare A, Cuocci C, Giacovazzo C, et al.: EXPO2013: a kit of tools for phasing crystal structures from powder data. J Appl Crystallogr. 2013, 46:1231-35. 10.1107/s0021889813013113
36. Sun J, Tian L, Yu Z, et al.: Studies on the size effects of nano-TiO2 on Portland cement hydration with different water to solid ratios. Constr Build Mater. 2020, 259:120390. 10.1016/j.conbuildmat.2020.120390
37. Feng D, Xie N, Gong C, et al.: Portland cement paste modified by TiO2 nanoparticles: a microstructure perspective. Ind & Eng Chem Res. 2013, 52:11575-82. 10.1021/ie4011595
38. Daniyal M, Akhtar S, Azam A: Effect of nano-TiO2 on the properties of cementitious composites under different exposure environments. J Mater Res Technol. 2019, 8:6158-72. 10.1016/j.jmrt.2019.10.010
39. Cerro-Prada E, García-Salgado S, Quijano MÁ: Controlled synthesis and microstructural properties of Sol-Gel TiO2 nanoparticles for photocatalytic cement composites. Nanomaterials. 2018, 9:26. 10.3390/nano9010026
40. Reddy NA, Chandana PS.: Microstructural analysis and densification of ordinary Portland cement mortars incorporated with minimal nano-TiO2: intermixing and surface coating on both fresh and hardened surfaces. Discov Mater. 2024, 4:28. 10.1007/s43939-024-00096-4